Bacteriorhodopsin Folds through a Poorly Organized Transition State

Jonathan P. Schlebach,[†,‡,#] Nicholas B. Woodall,[§,#] James U. Bowie,*[,§] and Chiwook Park*[,†,‡,||]

[†]Department of Medicinal Chemistry and Molecular Pharmacology, Purdue University, 575 Stadium Mall Drive, West Lafayette, Indiana 47907, United States

[‡]Interdisciplinary Life Science Graduate Program, Purdue University, 155 South Grant Street, West Lafayette, Indiana 47907, United States

[§]Department of Chemistry and Biochemistry, University of California, Los Angeles, 607 Charles E. Young Drive East, Box 951569, Los Angeles, California 90095-1569, United States

[||]Bindley Bioscience Center, Purdue University, 1203 West State Street, West Lafayette, Indiana 47907, United States

S *Supporting Information*

ABSTRACT: The folding mechanisms of helical membrane proteins remain largely uncharted. Here we characterize the kinetics of bacteriorhodopsin folding and employ φ-value analysis to explore the folding transition state. First, we developed and confirmed a kinetic model that allowed us to assess the rate of folding from SDS-denatured bacteriorhodopsin (bR_U) and provides accurate thermodynamic information even under influence of retinal hydrolysis. Next, we obtained reliable φ-values for 16 mutants of bacteriorhodopsin with good coverage across the protein. Every φ-value was less than 0.4, indicating the transition state is not uniquely structured. We suggest that the transition state is a loosely organized ensemble of conformations.
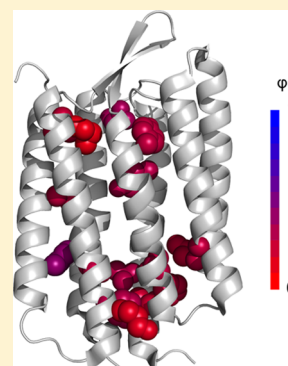
INTRODUCTION

To understand membrane protein folding, it is important to explore the nature of the transition state in the folding process. Φ-value analysis discerns the structure of the transition state by determining whether individual residues have their native contacts or not in the transition state.[1] Destabilizing point mutations are introduced by deleting interactions made in the folded state and the φ-value measures what fraction of the total destabilization also occurs in the transition state. When $\varphi = 1$, the full destabilization seen in the folded state is also realized in the transition state, suggesting that the side chain makes the same interactions in the transition state as in the native state. In other words, that part of the protein is structured in the transition state. Alternatively, when $\varphi = 0$, it implies that the mutated side chain has no effect on transition-state stability and therefore does not have native-like contacts in the transition state. By measuring φ-values for many residues, it is possible to map the transition state structure.

Although Φ-value analysis has been used extensively to study the folding of small water-soluble proteins,[2−8] the applications to membrane proteins have been limited. The Radford and Brockwell groups obtained extensive φ-values for the coupled folding/insertion of the β-barrel outer membrane protein PagP.[9] Their results suggest that the protein inserts via a partially folded structure that is tilted sideways with respect to the membrane normal. Otzen obtained φ-values for the helical membrane protein DsbB, suggesting the early formation of structure near the tips of several transmembrane helices may nucleate a wave of structure formation.[10] Previously, the mechanism of bR folding has been studied with unfolded bacterioopsin (bO) as the initial state.[11−14] Folding from unfolded bO involves formation of multiple intermediates and binding of retinal, which makes the kinetics unsuitable for φ-value analysis of a single transition state. However, refolding from unfolded bR (bR_U), which still retains retinal, occurs with a single dominant rate-limiting step and allows investigation of the transition state by φ-value analysis. Using this approach, the Booth group obtained φ-values for two helices in bR.[15,16] These results indicated that helix B is structured in the transition state, forming a nucleus for consolidation of the rest of the protein structure.

Subsequent to the initial φ-value analyses of bR folding, we found that the kinetics of bR folding was significantly altered by bulk solution concentrations of detergent,[17] which would likely confound φ-value measurements. For folding studies of bR, the protein is commonly solubilized in mixed micelles composed of a phospholipid (DMPC), a nondenaturing detergent (CHAP-SO or CHAPS) and various concentrations of the denaturing detergent SDS to alter the stability of the protein. The native

bR (bR$_F$) unfolds to SDS-denatured bR (bR$_U$) in a sigmoidal transition as the concentration of SDS is increased. Similarly, bR$_U$ refolds to bR$_F$ as the SDS concentration is decreased. Since the protein folds within a micelle environment, it is typical to express SDS concentration as the mole fraction of total detergent (X_{SDS}). The X_{SDS} can be readily adjusted to unfold the protein by adding more total SDS or to refold the protein by adding more total DMPC/CHAPSO or DMPC/CHAPS. When folding and unfolding kinetic measurements are performed in this way the bulk detergent concentration changes, however. Much to our surprise, we found that a higher DMPC/CHAPSO concentration increases the folding rate of bR by an unknown mechanism.[17] Thus, if one refolds bR by dilution from high X_{SDS} into low X_{SDS} by simply adding a high concentration of DMPC/CHAPSO, the folding rate will increase as X_{SDS} is lowered by both the increased stability of the folded state and also the higher DMPC/CHAPSO concentration. As a result, the sensitivity of the rate constants with X_{SDS} will be a complex function of both folding and detergent properties.

Given the unexpected discovery of the detergent dependence on folding rates,[17] we remeasured a few key φ-values holding the total DMPC/CHAPSO concentration constant. Our initial results deviated substantially from the prior measurements. We therefore repeated and further extended the φ-value analysis to obtain a more comprehensive view of the transition state for bR folding.

■ RESULTS AND DISCUSSION

Model for bR Folding Kinetics. Increasing the mole fraction of SDS results in the conversion of bR$_F$ to a bR$_U$ state, which we refer to as unfolding. In the bRu state, tertiary structure is lost, but most of the secondary structure remains.[18] The characteristic absorbance of the retinal cofactor in native bR serves as a convenient probe to follow this transition in the protein. Yet the cofactor can also complicate efforts to investigate the folding of this protein. When bR$_F$ is unfolded to bR$_U$, the retinal Schiff base is susceptible to hydrolysis, which results in the formation of bacterioopsin (bO). Therefore, the complete reaction of bR unfolding occurs as shown in Scheme 1, where k_f, k_u, and k_h are the rate constants for folding,

Scheme 1

$$bR_F \underset{k_f}{\overset{k_u}{\rightleftarrows}} bR_U \xrightarrow{k_h} bO + retinal$$
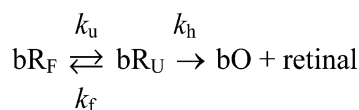
unfolding, and hydrolysis, respectively. Retinal hydrolysis is reversible but can be treated as irreversible for simplicity in the range of X_{SDS} where the equilibrium between bR$_F$ and bR$_U$ is investigated.[17] In this kinetic scheme, the equilibrium between bR$_F$ and bR$_U$ can be achieved experimentally only when the conformational relaxation is much faster than retinal hydrolysis ($k_u + k_f \gg k_h$). We previously demonstrated that bR folding is significantly faster in 29 mM DMPC and 31 mM CHAPSO than in 15 mM DMPC and 16 mM CHAPSO (or CHAPS),[17] which is the typical condition previously employed for the investigation of folding energetics of bR.[14−16,19,20] Faster folding of bR in 29 mM DMPC and 31 mM CHAPSO is beneficial in suppressing the influence of the retinal hydrolysis on the folding kinetics. However, even in 29 mM DMPC and

31 mM CHAPSO, retinal hydrolysis still interferes with the folding and unfolding of bR in the transition zone. Therefore, the hydrolysis reaction must be accounted for as shown in Scheme 1 in order to determine the rate constants for folding and unfolding.

When the folding and unfolding of bR occurs as shown in Scheme 1, the concentration of bR$_F$ is expressed as a function of time in a double-exponential equation:[21]

$$[bR_F] = a_1 e^{-\lambda_1 t} + a_2 e^{-\lambda_2 t} \tag{1}$$

where λ_1 and λ_2 are the macroscopic rate constants and a_1 and a_2 are the amplitudes for the fast phase and the slow phase, respectively. According to the kinetic model in Scheme 1, λ_1 and λ_2 are the solutions of the following quadratic equation (see Supporting Information):[21]

$$\lambda^2 - (k_f + k_u + k_h)\lambda + k_u k_h = 0 \tag{2}$$

Whether folding or unfolding is monitored, the change in bR$_F$ concentration is described with the same rate constants, λ_1 and λ_2. According to the initial conditions, $a_1 + a_2$ is zero for a folding reaction or the initial total bR$_F$ concentration for an unfolding reaction.

On the basis of the property of a quadratic equation, we can extract the relationship between the macroscopic rate constants, λ_1 and λ_2, and the three elementary rate constants for folding, unfolding, and hydrolysis from eq 2 as follows:

$$\lambda_1 \lambda_2 = k_u k_h \tag{3}$$

$$\lambda_1 + \lambda_2 = k_f + k_u + k_h \tag{4}$$

From these identities, the rate constants for folding and unfolding under a given condition can be extracted from the experimentally determined values of λ_1, λ_2, and k_h. The relative amplitudes of the two phases observed in folding and unfolding reactions (a_1 and a_2 in eq 1) are also dependent on k_f and k_u, but we did not use the amplitudes in determining k_f and k_u due to the limited accuracy with which the amplitudes could be determined.

Validation of the Kinetic Model. To assess whether the observed relaxation kinetics are consistent with the kinetic model (Scheme 1), we first investigated the folding and unfolding of bR in 29 mM DMPC and 31 mM CHAPSO at $X_{SDS} = 0.73$. At this X_{SDS}, bR$_F$ shifts instantaneously to a previously described 600 nm "blue form" before slowly unfolding to the SDS-denatured state at 440 nm.[14] The rapid shift does not interfere with our kinetic measurements that are taken over the course of 2 h. The 600 nm "blue form" likely results from the protonation of D85 and the isomerization of the retinal cofactor[14] which only negligibly alters both the structure and energetics compared to the unfolding of bacteriorhodopsin. Data collected at both 560 and 600 nm gives indistinguishable kinetic rates.

As shown in Figure 1A, refolding features an initial increase in A_{600} followed by a slow decay driven by retinal hydrolysis as expected from our kinetic model. Unfolding also features two kinetic phases, which is obvious from nonrandom curve fitting residuals for a single exponential fit (Figure S1). The time scale of the slow phase is similar to the time scale of retinal hydrolysis ($t_{1/2} \sim 10$ min),[14,17] suggesting that the biphasic kinetics result from retinal hydrolysis, consistent with the model in Scheme 1.

On the basis of this kinetic model, we determined λ_1 and λ_2 of wild-type bR at varying X_{SDS} using both refolding and
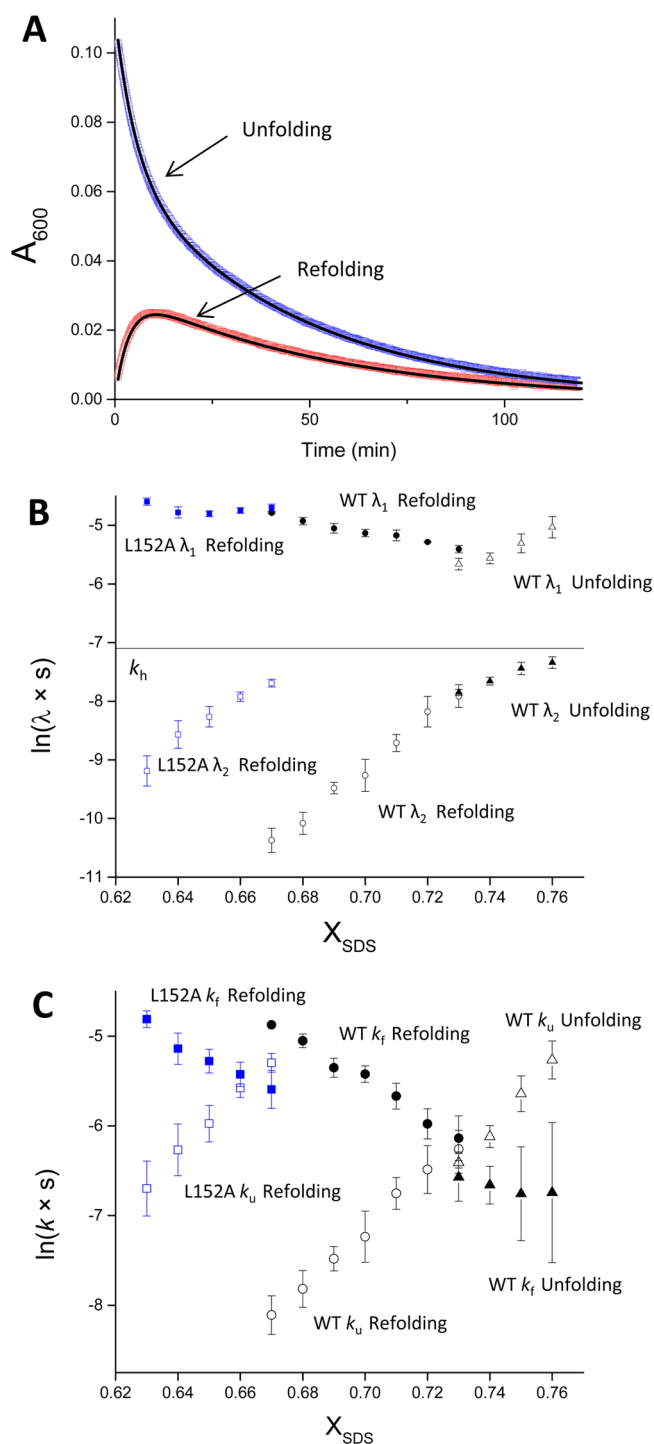
Figure 1. Conformational relaxation kinetics of bR in the folding transition zone. (A) The refolding of bR_U (red) and unfolding of bR_F (blue) monitored at $X_{SDS} = 0.73$ by the absorbance of the folded protein at 600 nm (A_{600}). The curve-fitting of the change of A_{600} with eq 1 is shown in black lines. (B) Dependence of the observed rate constants on X_{SDS}. The natural logarithms of the rate constants of the fast (λ_1) and slow (λ_2) phases of conformational relaxation of wild-type (black) and L152A (blue) bR's are plotted against X_{SDS}. Whether the values were obtained from unfolding or refolding is indicated in the figure. The rate of retinal hydrolysis (k_h; black line) is plotted for reference. (C) Dependence of the folding and unfolding rate constants on X_{SDS}. The natural logarithms of the rate constants for folding (k_f) and for unfolding (k_u) of wild-type (black) and L152A (blue) bR's are plotted against X_{SDS}. Whether the values were obtained from unfolding or refolding is indicated in the figure.

unfolding reactions ($X_{SDS} = 0.67-0.76$) (Figure 1B). When plotted against X_{SDS}, the natural logarithm of the observed rates constants (ln λ_1 and ln λ_2) make a continuous trend throughout the entire range of X_{SDS}. As predicted by eq 2 (see Supporting Information), λ_1 is greater than k_h, and λ_2 is less than k_h. The kinetic model predicts that the λ_1 and λ_2 values observed in the folding reaction are identical to those observed in the unfolding reaction at the same X_{SDS}. At $X_{SDS} = 0.73$, where both folding and unfolding can be monitored, we found λ_1 and λ_2 to be (4.5 ± 0.3) × 10^{-3} s^{-1} and (3.7 ± 0.8) × 10^{-4} s^{-1}, respectively, when measured in the folding direction and (3.5 ± 0.3) × 10^{-3} s^{-1} and (3.7 ± 0.2) × 10^{-4} s^{-1}, respectively, when measured in the unfolding direction (Figure 1B). The similarity in the kinetic constants is consistent with the model of folding under the influence of retinal hydrolysis.

Using eqs 3 and 4, we calculated k_f and k_u values from the experimentally determined λ_1 and λ_2 within the transition zone from the chevron plots shown in Figure 1B. We determined k_h experimentally to be (8.3 ± 0.4) × 10^{-4} s^{-1} by monitoring free retinal release from bR_U at $X_{SDS} = 0.83$ (Figure S2). As seen in Figure 1C, the ln k_f and ln k_u values are, within experimental error, linearly dependent on X_{SDS} in the transition zone of the equilibrium unfolding curves ($X_{SDS} = 0.67-0.76$). The values for k_f obtained from unfolding kinetic traces are particularly unreliable because the error in the k_f measurement originates from both the error in k_u and in k_h. Consequently, when k_f is small, the absolute errors in both the larger k_u and k_h values overwhelm the measurement.

The kinetic model predicts that the kinetic C_m value, where the k_f and k_u are equal, should be the same when the values are obtained from the folding reaction or the refolding reaction. Indeed, the kinetic C_m value for wild-type bR (the intersection of the linear fits of ln k_f and ln k_u) is 0.73 in X_{SDS} when the values are obtained from refolding experiments and 0.73 in X_{SDS} when the parameters are obtained by unfolding experiments. Overall, the kinetic scheme fits the observed behavior well.

Effect of Mutations on Kinetics of bR Folding. To survey the effect of mutations on the folding kinetics of bR, we tested 30 mutations of buried residues. For each mutant, we determined kinetic parameters at a range of X_{SDS} around the transition zone. The dependence of ln k_u and ln k_f were generally well described by linear fits. The mutations L66A, F71A, D115A, R134A, W138A, S141A, M145A, and L149A did not destabilize bR more than 0.5 kcal/mol according to our kinetic measurements and therefore were not suitable for φ-value analysis. Other mutations appeared to alter the folding pathway of bR precluding the application of φ-value analysis. For example, the $m_{\ddagger-u}$ for the mutants I119A and L93A, T47A were near zero (Figure S3). Such a drastic change in the response to denaturant implies an altered folding pathway. Mutants L94A, W86F, I148A, W189F, and F219A displayed altered kinetic traces as compared to the wild-type bR (Figure S4). Specifically, our kinetic model predicts that the irreversible hydrolysis of retinal in the transition zone of bR_F to bR_U will eventually convert all the protein to bO, but these mutants had a significant residual absorbance that lasted for many hours, perhaps reflecting residual structure in the unfolded state. In the end, we chose 16 bR mutants that we considered suitable for φ-value analysis. An example (L152A bR) is shown in Figure 1B and 1C, and all the chevron plots are present in Figure S5. The results from the kinetic analysis of the selected mutants are summarized in Table 1.

Table 1. Folding and Unfolding Kinetics of Bacteriorhodopsin and Its Mutants

	φ_F	$\Delta\Delta G_{unf}^{okin\,a}$ (kcal/mol)	$\Delta\Delta G_{unf}^{oeq\,b}$ (kcal/mol)	$m_{\ddagger\text{-}u}$ (kcal/mol)	$m_{\ddagger\text{-}f}$ (kcal/mol)	m_{kin}^{c} (kcal/mol)	k_f^{d} ($\times10^{-3}$ s^{-1})	k_u^{d} ($\times10^{-3}$ s^{-1})
WT	–	–	–	-12.8 ± 0.7	18.9 ± 0.7	31.7 ± 0.9	7.8 ± 1.0	0.3 ± 0.03
L13A	0.23 ± 0.06	-1.8 ± 0.2	-1.3 ± 0.1	-15.0 ± 0.7	27.4 ± 1.9	42.3 ± 2.0	3.8 ± 0.3	3.1 ± 0.7
M20A	0.25 ± 0.06	-2.8 ± 0.5	-2.7 ± 0.1	-7.8 ± 0.4	19.2 ± 2.8	27.0 ± 2.8	2.4 ± 0.3	10.8 ± 0.9
F27A	0.43 ± 0.07	-2.1 ± 0.2	-2.2 ± 0.2	-14.1 ± 0.7	17.7 ± 1.3	31.8 ± 1.4	1.7 ± 0.2	2.3 ± 0.6
K41A	0.13 ± 0.12	-0.9 ± 0.2	-0.7 ± 0.1	-12.6 ± 1.2	25.1 ± 0.7	37.7 ± 1.3	6.4 ± 0.8	1.1 ± 0.1
F42A	0.29 ± 0.10	-2.1 ± 0.4	-1.8 ± 0.1	-12.3 ± 1.8	14.4 ± 2.7	26.7 ± 3.3	2.8 ± 0.8	3.7 ± 1.6
T46A	0.26 ± 0.09	-2.2 ± 0.5	-2.3 ± 0.1	-11.2 ± 0.7	12.6 ± 2.2	23.8 ± 2.2	3.0 ± 0.7	4.7 ± 3.5
M60A	0.10 ± 0.14	-1.1 ± 0.3	-1.1 ± 0.1	-17.4 ± 2.1	15.6 ± 3.6	33.0 ± 4.2	6.6 ± 1.4	1.6 ± 0.5
Y83A^e	0.25 ± 0.10	-1.7 ± 0.4	-0.8 ± 0.1	-14.3 ± 0.6	15.6 ± 1.9	29.9 ± 2.0	3.9 ± 0.8	2.4 ± 1.1
L97A	0.26 ± 0.08	-2.9 ± 0.4	-2.4 ± 0.1	-11.2 ± 1.1	33.4 ± 1.3	44.6 ± 1.7	2.2 ± 0.7	12 ± 5
L100A	0.20 ± 0.07	-3.2 ± 0.3	-2.9 ± 0.2	-9.9 ± 1.2	21.2 ± 1.1	31.1 ± 1.6	2.7 ± 0.9	22 ± 8
L111A	0.25 ± 0.07	-2.0 ± 0.3	-1.8 ± 0.1	-10.8 ± 1.7	27.7 ± 1.9	38.4 ± 2.5	3.3 ± 0.6	3.6 ± 1.0
L152A	0.21 ± 0.06	-2.1 ± 0.2	-1.6 ± 0.1	-10.4 ± 1.1	20.1 ± 0.9	31.2 ± 1.4	3.7 ± 0.5	5.2 ± 0.8
F171A	0.23 ± 0.09	-1.1 ± 0.2	-0.9 ± 0.1	-8.7 ± 1.2	21.5 ± 1.5	30.2 ± 1.9	5.1 ± 0.4	1.3 ± 0.1
L174A	0.28 ± 0.16	-1.8 ± 0.4	-1.8 ± 0.1	-12.8 ± 3.9	9.2 ± 3.2	22.0 ± 5.0	3.4 ± 1.4	2.5 ± 1.0
Y185A^f	0.29 ± 0.08	-4.2 ± 0.5	-2.9 ± 0.1	-13.6 ± 1.4	23.1 ± 1.8	36.7 ± 2.2	1.0 ± 0.5	47 ± 30
E204A	0.34 ± 0.08	-2.2 ± 0.3	-1.8 ± 0.1	-8.1 ± 0.6	15.8 ± 1.6	24.0 ± 1.7	2.2 ± 0.3	3.4 ± 1.5

$^a\Delta\Delta G_{unf}^{okin}$ values were calculated from k_f and k_u at $X_{SDS} = 0.67$ using eq 6. $^b\Delta\Delta G_{unf}^{oeq}$ values are the stability of bR determined with bO as the reference state. $^c m_{kin} = m_{\ddagger\text{-}f} - m_{\ddagger\text{-}u}$. ^{d}Kinetic constants at $X_{SDS} = 0.67$ ^{e}Mutation shifted λ_{max} to 520 nm in DMPC/CHAPSO. ^{f}Mutation shifted λ_{max} to 530 nm in DMPC/CHAPSO.

Tanford β Value. The slopes of the plots of ln k_f ($m_{\ddagger\text{-}u}$) and ln k_u ($m_{\ddagger\text{-}u}$) versus X_{SDS} are measures of the protein's sensitivity to denaturant, and reflect how close in their interaction with SDS the folding transition state is to the folded or unfolded state on the reaction coordinate. For wild-type bR $m_{\ddagger\text{-}u} = -12.8 \pm 0.7$ kcal/mol and $m_{\ddagger\text{-}n} = 18.9 \pm 0.7$ kcal/mol. The slope in the unfolding direction is larger than the slope in the folding direction, indicating that the transition state is closer to the unfolded state. This is generally quantified by the Tanford β-value:

$$\beta = \frac{m_{\ddagger\text{-}u}}{m_{\ddagger\text{-}u} - m_{\ddagger\text{-}u}}$$

We obtain a β-value of 0.4, suggesting that the transition state for unfolding is a little more than halfway to the fully unfolded protein. This value contrasts with the previously determined β-value of 0.1,[15] most likely because the slopes were previously altered by the changing detergent concentrations. The previous study also reported that β-values of bR mutants correlate with the change in the energy of the transition state ($\Delta\Delta G_{\ddagger\text{-}U}$), indicating the movement of the transition state along the reaction coordinate upon destabilization of the protein.[16] However, we do not observe any significant correlation either between the β-values and $\Delta\Delta G_{\ddagger\text{-}U}$ or between the kinetic m-values and $\Delta\Delta G_{unf}°$ (Figure S6). The lack of the dependence suggests that destabilization of the native structure by mutations does not alter the degree of the interaction between the transition state and SDS relative to bR$_F$ and bR$_U$.

Correspondence of Kinetic and Equilibrium Measurements. The ratio of the rate constants k_u/k_f corresponds to the equilibrium constant for the bR$_F$ to bR$_U$ transition, K_{unf}(bR). To further validate the model, it would be useful to compare the equilibrium constant calculated with the rate constants with the value obtained from equilibrium measurements. Direct comparison of kinetically inferred equilibrium constants to experimentally determined equilibrium constants is not possible, however, because the bR$_F$ to bR$_U$ transition is not

fast enough to eliminate the interference from retinal hydrolysis.[22] Nevertheless, we can obtain the equilibrium constant, K_{unf}(bO), for the overall reaction:[22] bR$_F$ $\rightleftharpoons$ bO + retinal. We therefore decided to compare the mutational effects on K_{unf}(bO) from equilibrium measurements with their effects on K_{unf}(bR) obtained from kinetics. Since linear free energy relationships do not appear to hold over a large range of X_{SDS},[23] we wanted to minimize extrapolations. We therefore compare values at $X_{SDS} = 0.67$, near the lower edge of the transition zone for the wild-type protein. Since all the mutants in this work destabilize the protein, this is a point where we can generally either make a direct measurement or where only a short extrapolation is required.

For the mutants used in φ-value analysis, we compared $\Delta\Delta G_{unf}°$ obtained by kinetics with those obtained from the equilibrium measurements. As shown in Figure 2, we see a linear correlation with a slope of 0.97, very close to ideal expected slope of 1.00. The close agreement despite a difference in reference state and a large shift in C_m between the two methods further supports the validity of our kinetic model.

Φ-Value Analysis of Bacteriorhodopsin. With the kinetic model that can reliably determine k_f and k_u for bR, we set out to map the transition state of folding by φ-value analysis. Φ-values are the ratio of the change in free energy of the transition state upon mutation, $\Delta\Delta G_{\ddagger\text{-}U}$, (derived from k_f) to $\Delta\Delta G_{unf}°$ (here derived from k_f and k_u). The ideal mutation for φ-value analysis destabilizes the protein by at least 1 kcal/mol to provide sufficient signal-to-noise,[24] without introducing any new interactions or altering the kinetic behavior.[1] The mutants for which we have determined φ-values (Table 1) were selected based on these criteria. Also, for φ-value determination we used kinetic constants at $X_{SDS} = 0.67$, which either required no extrapolation or only small extrapolations from the experimentally observable range of X_{SDS}.

The 16 reliable φ-values provide good coverage across the protein (Figure 3). Including the residues that make interhelical contacts with the mutated residues, this analysis covers the
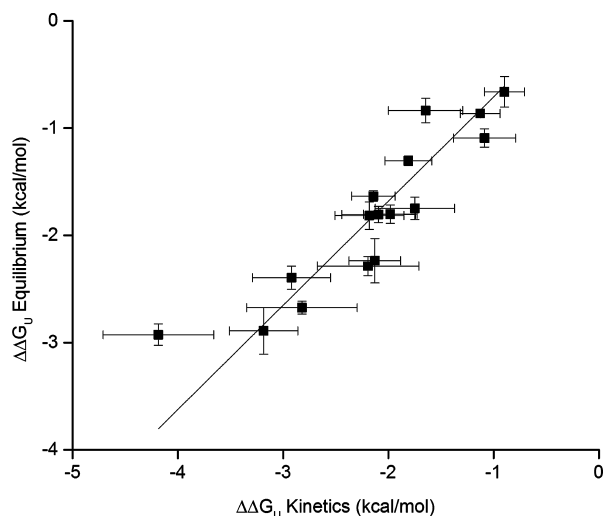
Figure 2. Comparison of $\Delta\Delta G_{unf}°(bR)$ from kinetics to $\Delta\Delta G_{unf}°(bO)$ from equilibrium measurements. The effect of mutation on the free energy of unfolding as measured via the kinetic model to the bR_U reference state or obtained from equilibrium methods to the bO reference state. A weighted linear fit to the data is shown (slope = 0.97, intercept = 0.26 kcal/mol, R^2 = 0.88).

structure of bR extensively. The mutations that are excluded from φ-values do not show any apparent pattern in their distribution on the structure (Figure 3B), which indicates that our survey is not biased to a specific region by their exclusion. Every φ-value measured was low. In particular, 14 of the 16 φ-values measured were at or below 0.3 and the other two (F27A and E204A) were ~0.4.

The globally distributed low φ-values indicate that development of a localized folding nucleus in the transition state is not likely. Even the two residues with relatively higher φ-values are distant from each other in the native structure, unlikely to coalesce in a folding nucleus. Considering most of the mutated residues contain extensive interhelical contacts in the native structure, we can picture that interhelical packing is minimal in the transition state. These results suggest that there is not a high degree of unique structure in the transition state.

Mechanism of Folding from SDS-Denatured Bacteriorhodopsin. The kinetics of refolding from the bO state has been investigated in the pioneering spectroscopic studies of the Booth group[12,13,25,26] and more recently by elegant studies by the Lanyi group[27] using EPR methods and the Konermann group using pulsed oxidation or H/D exchange reactions.[28,29] All see a series of intermediate states prior to the slow incorporation of retinal. In our case, however, we are examining
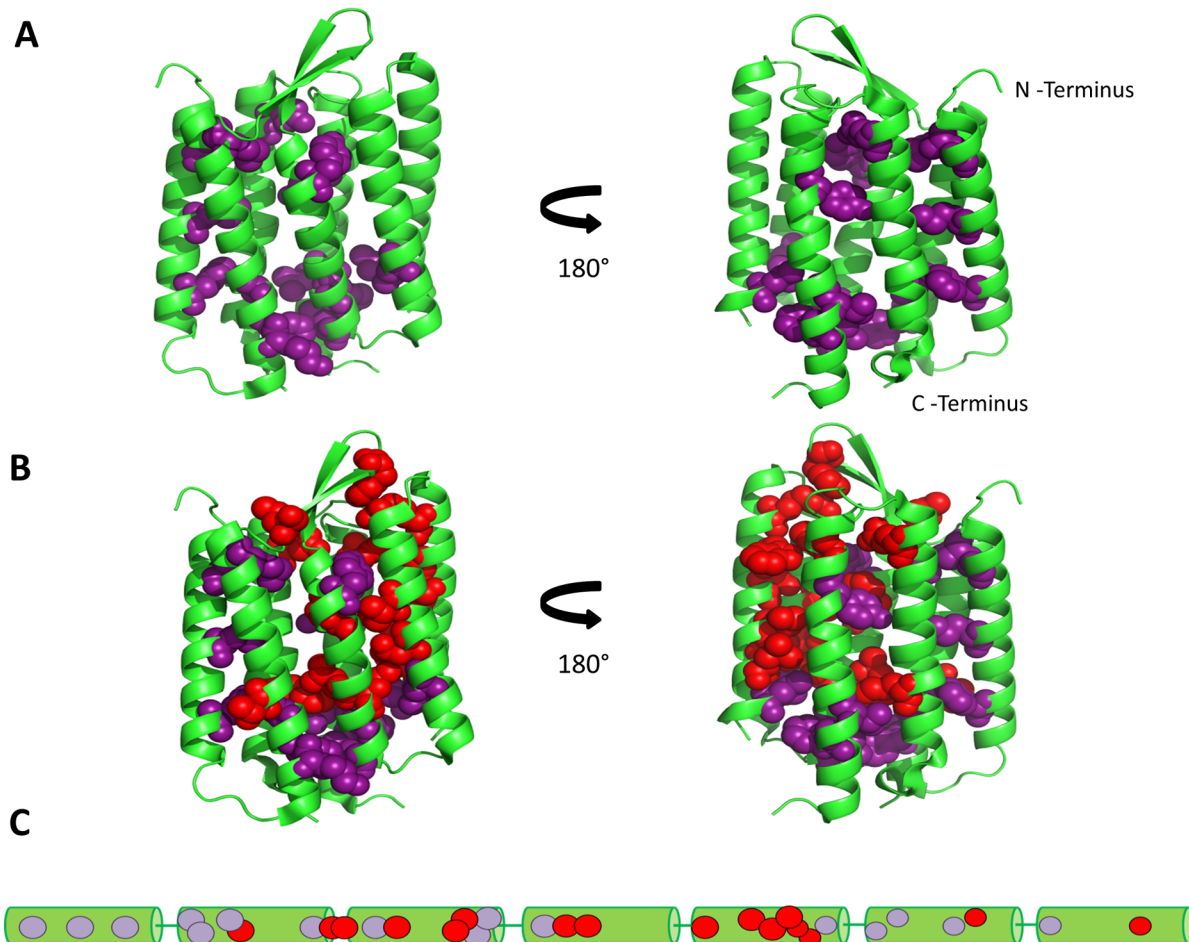

Figure 3. Φ-value map of bR. (A) The side chains of the 16 positions where we obtained reliable φ-values are shown in purple on the structure of bR (PDB 1C3W[32]). The backbone trace is shown as a green ribbon. (B) The side chains of the positions that did not yield usable φ-values are shown in red, along with the side chains of positions that did yield useable φ-values in purple. (C) The positions are shown on a secondary structure map below using the same color scheme in panels A and B.

folding from the bR$_U$ state for which the retinal is already covalently attached. Folding from bR$_U$ is less complex and is well described by a two-state model[14,22] as in Scheme 1.

The structure of bR$_U$ in SDS has been investigated by the Lanyi and Langen laboratories using DEER spectroscopy.[18] Their results indicate that the transmembrane helix structure remains, but is heterogeneously frayed, consistent with the ~40% reduction in helical content seen by far-UV CD spectroscopy.[11] Results from the Konermann group using pulsed H/D exchange are also consistent with fluctuating helical secondary structure.[29] In contrast, the tertiary structure is largely lost in the SDS unfolded state. Thus, folding of bR from an SDS denatured state (bR$_U$) involves the assembly of largely preformed transmembrane helices as envisioned in the two-stage model of helical membrane protein folding.[30] But how does this assembly occur?

Globally distributed low φ-values indicate that bR does not have significant interhelical packing in the transition state. On the basis of our results, we envision an expanded, poorly ordered transition state in which partially folded, fluctuating transmembrane helices have roughly correct orientation/topology and are ready to coalesce in a cooperative fashion. This model is similar to the topomer search model proposed for soluble proteins.[31] While achieving an approximately topologically correct structure at random without any energetic guidance from native contacts is somewhat improbable, finding this state would be facilitated by the short loops of bR and the largely preformed helices. If achieving a topologically correct structure is the rate-limiting step, the energetic barrier to reach the transition state would be largely entropic. Reducing the search space significantly, the short loops and the preformed helices may decrease the entropic cost to achieve the topologically correct transition state.

Another structural change we may envision to occur in the transition state is shedding of SDS molecules. The β-value of 0.4 indicates that interaction with SDS in the transition state is somewhat distinct from that in the unfolded state. In the bR$_U$ state, SDS is believed to interact with individual helices extensively. The lack of native-like contacts in the transition state suggests that some SDS may still remain between helices in the transition state.

The low fractional φ-values may also result from a number of relatively iso-energetic pathways. In this case, the transition state is an ensemble of structures that contain native-like interhelical contacts at different locations. It is easy to envision a folding mechanism involving an initial collection of helices as the transition state followed by the rapid accrual of the additional helices. Such a mechanism could occur by many different pathways. To have similar low φ-values throughout the protein structure, however, each pathway needs to contribute equally to the overall folding of bR, which is somewhat hard to imagine considering the cooperative nature of protein folding in general.

CONCLUSIONS

Refolding of bacteriorhodopsin from the SDS-denatured bR$_U$ state offers a valuable opportunity to investigate folding of helical membrane proteins in a great detail. Though retinal hydrolysis complicates the kinetics, we demonstrate here that using a proper kinetic model we can reliably determine folding and unfolding kinetic parameters. Refolding to bR$_F$ followed by slow retinal hydrolysis allowed us to determine folding and unfolding kinetic constants simultaneously in an extended

region near the transition zone (Figure 1C), which is not possible in most proteins. We confirmed the validity of the kinetic model and the folding and unfolding kinetic constants from the model by comparing k_f and k_u determined from unfolding reactions and those determined from folding reactions (Figure 1A) and also by comparing $\Delta\Delta G_{unf}°$ values determined from kinetics with those determined from equilibrium unfolding.

Our φ-value analysis of the bR$_U$-to-bR$_F$ transition indicates that the structure of the transition state is poorly organized without any significant interhelical native contacts. This finding is distinct from the previous report of helix B being the folding nucleus of bR folding,[16] demonstrating the importance of eliminating the effect of the change in detergent concentrations on folding rates. With the comprehensive φ-value analysis, bR is a rather unique membrane protein since we now have considerable structural information about the folded state,[32] the unfolded state,[18] and the transition state. On the basis of the known structure of bR$_U$ and our φ-value analysis, we propose that the rate-limiting step of bR refolding from SDS-denatured form is finding the topologically correct helical arrangement from the ensemble of rapidly interconverting conformations with largely preformed helices. As the orientation of the transmembrane helices is limited in a bilayer, bR may not have this topology search problem under natural conditions. Thus, it is possible that the folding transition state is different under native conditions, but investigation of that possibility will require developing new technology for studying the folding process in bilayers.[23,33]

EXPERIMENTAL SECTION

Materials. Wild-type and mutant bR's were expressed and purified as previously described.[34−36] 1,2-Dimyristoyl-sn-glycerol-3-phosphocholine (DMPC) was purchased from Avanti Polar Lipids (Alabaster, AL). 3[(3-cholamidopropyl)dimethylammonio]-2-hydroxy-1-propane-sulfonate (CHAPSO) was purchased from Affymetrix (Maumee, OH). Bio-Xtra sodium dodecyl sulfate was purchased from Sigma-Aldrich.

Refolding Kinetics. The bR protein was equilibrated in 10 mM sodium phosphate buffer (pH 6.0) containing 15 mM DMPC and 16 mM CHAPSO at 25 °C for at least an hour prior to refolding experiments. The protein was first unfolded by incubating 1.0 mg/mL bR in 10 mM sodium phosphate buffer (pH 6.0) containing 15 mM DMPC/16 mM CHAPSO and SDS at X_{SDS} = 0.82 at room temperature for 3 min. Refolding was then initiated by diluting 10-fold into a 10 mM sodium phosphate buffer (pH 6.0) containing varying concentrations of SDS, DMPC, and CHAPSO at 25 °C. The final refolding reactions contained 29 mM DMPC, 31 mM CHAPSO and 0.10 mg/mL bR. The absorption at 600 nm was monitored on a Molecular Devices Spectra Max M5 plate reader for 2 h. The rate constants for each refolding reaction were determined by fitting a plot of the A_{600} versus time to eq 1. Because folding and unfolding rate constants are not sensitive to small differences in k_h (data not shown), we assumed k_h in the mutants is the same as that of wild-type bR. Mutants Y83A and Y185A had altered λ_{max} values of 520 and 530 nm, respectively, when solubilized in DMPC/CHAPSO. The absorption at 560 nm was used to monitor the refolding of these mutants.

Unfolding Kinetics. bR was equilibrated in 10 mM sodium phosphate buffer (pH 6.0) containing 15 mM DMPC and 16 mM CHAPSO at 25 °C for at least an hour prior to unfolding. Unfolding was initiated at 25 °C by a 10-fold dilution into a 10 mM sodium phosphate buffer (pH 6.0) containing 30 mM DMPC, 32 mM CHAPSO, and varying concentrations of SDS. The final unfolding reactions contained 29 mM DMPC and 31 mM CHAPSO. The final protein concentration was 0.10 mg/mL. The absorption at 600 nm was monitored on a Molecular Devices Spectra Max M5 plate reader

for 2 h. Observed rate constants for each unfolding reaction were determined by fitting a plot of the A_{600} versus time according to eq 1.

Determination of Consensus Values for the Observed Rate Constants in the Transition Zone. To ensure accurate determination of λ_1 and λ_2 for bR, we measured the kinetic constants for both folding and unfolding reactions in triplicate within a range of X_{SDS} near the C_m. We calculated k_f and k_u from λ_1, λ_2, and k_h using eqs 3 and 4. For k_h, we use $(8.3 \pm 0.4) \times 10^{-4}$ s^{-1}, which we determined by monitoring free retinal release from wild-type bR$_U$ at $X_{SDS} = 0.83$. We assumed mutations do not affect k_h. To validate this assumption, we investigated the kinetics of hydrolysis step of two mutants. The k_h values of L111A bR and E204A bR were $(7.5 \pm 0.2) \times 10^{-4}$ s^{-1} and $(7.7 \pm 0.6) \times 10^{-4}$ s^{-1}, respectively, which were not significantly different from that of wild-type bR, $(8.3 \pm 0.4) \times 10^{-4}$ s^{-1}. Moreover, the use of the individual k_h values does not affect the φ-values. The dependence of the natural logarithm of k_f on the X_{SDS} ($m_{\ddagger-u}$) and the natural logarithm of k_u on the X_{SDS} ($m_{\ddagger-f}$) were determined by fitting the linear portions of the natural logarithms of the consensus rate constants for folding and unfolding against the X_{SDS} in the transition zone.

Calculation of Phi Values. Φ-values are the ratio of the free energy change of the transition state upon mutation ($\Delta\Delta G_{\ddagger-U}$) to the free energy change of unfolding upon mutation ($\Delta\Delta G_{unf}°$).

$$\phi_F = \frac{\Delta\Delta G_{\ddagger-U}}{\Delta\Delta G_{unf}°}$$

$\Delta\Delta G_{\ddagger-U}°$ is calculated from the wild type and mutant folding rates as follows:

$$\Delta\Delta G_{\ddagger-U} = RT \ln \frac{k_f(\text{wt})}{k_f(\text{mut})} \tag{5}$$

$\Delta\Delta G_{unf}°$ is calculated from the wild type and mutant folding rates and unfolding rates as follows:

$$\Delta\Delta G_{unf}° = RT \ln \frac{k_f(\text{mut})}{k_u(\text{mut})} - RT \ln \frac{k_f(\text{wt})}{k_u(\text{wt})} \tag{6}$$

The k_u and k_f kinetic rates were calculated from the measured λ_1 and λ_2 values as described in the text. The value of k_u and k_f was interpolated or extrapolated to $X_{SDS} = 0.67$ using a weighted linear fit of $\ln(k_u)$ or $\ln(k_f)$ by the predict function in the R statistics program. These values were then used to calculate the φ-value. The error for the φ-value was propagated from the triplicate measurement of λ_1 and λ_2. The error for the interpolation or extrapolation to $X_{SDS} = 0.67$ used the 95% confidence interval for the predicted value.

Unfolding Equilibrium Measurements. The bR$_F$-to-bO$_U$ unfolding equilibrium was measured and calculated as described previously[22] except the conditions were altered to match the conditions used for the refolding kinetics of bR. The final conditions were 0.1 mg/mL bR, 30 mM DMPC, 32 mM CHAPSO, 10 mM sodium phosphate pH 6.0, 9.1 μM all-*trans* RET and varying SDS concentrations. After the samples were equilibrated in dark at room temperature for ~4 days in a 96-well UV-star microplate (Greiner Bio-One), the absorbance at 553 nm was measured by SpectraMax M5 plate reader (Molecular Devices). All measurements were done in triplicate.

ASSOCIATED CONTENT

Ⓢ Supporting Information

Derivation of eq 2. Proof that $\lambda_1 > k_h$ and $\lambda_2 < k_h$. Residuals from curve-fitting of bR unfolding. Kinetics of retinal hydrolysis. Refolding of F219A bR. The extracted rates constants of the bR mutants used for φ-value analysis. Lack of dependence of the folding and unfolding behavior of bR on the degree of destabilization upon mutation. This material is available free of charge via the Internet at http://pubs.acs.org.

AUTHOR INFORMATION

Corresponding Authors

bowie@mbi.ucla.edu
chiwook@purdue.edu

Author Contributions

#J.P.S. and N.B.W. contributed equally.

Notes

The authors declare no competing financial interest.

REFERENCES

(1) Serrano, L.; Matouschek, A.; Fersht, A. R. *J. Mol. Biol.* **1992**, *224*, 771.

(2) Itzhaki, L. S.; Otzen, D. E.; Fersht, A. R. *J. Mol. Biol.* **1995**, *254*, 260.

(3) Mayor, U.; Guydosh, N.; Johnson, C.; Grossman, J. G.; Sato, S.; Jas, G.; Freund, S.; Alonso, D.; Daggett, V.; Alan, F. *Nature* **2003**, *421*, 863.

(4) Daggett, V.; Li, A.; Itzhaki, L. S.; Otzen, D. E.; Fersht, A. R. *J. Mol. Biol.* **1996**, *257*, 430.

(5) Nickson, A. A.; Stoll, K. E.; Clarke, J. *J. Mol. Biol.* **2008**, *380*, 557.

(6) Riddle, D.; Grantcharova, V.; Santiago, J.; Alm, E.; Ruczinski, I.; Baker, D. *Nat. Struct. Biol.* **1999**, *6*, 1016.

(7) Chiti, F.; Taddei, N.; White, P. M.; Bucciantini, M.; Magherini, F.; Stefani, M.; Dobson, C. M. *Nat. Struct. Mol. Biol.* **1999**, *6*, 1005.

(8) Zarrineafsar, A. *Methods* **2004**, *34*, 41.

(9) Huysmans, G. H. M.; Baldwin, S. A.; Brockwell, D. J.; Radford, S. E. *Proc. Natl. Acad. Sci. U. S. A.* **2010**, *107*, 4099.

(10) Otzen, D. E. *J. Mol. Biol.* **2003**, *330*, 641.

(11) Riley, M. L.; Wallace, B. A.; Flitsch, S. L.; Booth, P. J. *Biochemistry* **1997**, *36*, 192.

(12) Booth, P.; Flitsch, S.; Stern, L.; Greenhalgh, D.; Kim, P.; Khorana, H. G. *Nat. Struct. Mol. Biol.* **1995**, *2*, 139.

(13) Booth, P. J.; Farooq, A.; Flitsch, S. L. *Biochemistry* **1996**, *35*, 5902.

(14) Curnow, P.; Booth, P. J. *Proc. Natl. Acad. Sci. U. S. A.* **2007**, *104*, 18970.

(15) Curnow, P.; Booth, P. J. *Proc. Natl. Acad. Sci. U. S. A.* **2009**, *106*, 773.

(16) Curnow, P.; Di Bartolo, N. D.; Moreton, K. M.; Ajoje, O. O.; Saggese, N. P.; Booth, P. J. *Proc. Natl. Acad. Sci. U. S. A.* **2011**, *108*, 14133.

(17) Schlebach, J. P.; Cao, Z.; Bowie, J. U.; Park, C. *Protein Sci.* **2012**, *21*, 97.

(18) Krishnamani, V.; Hegde, B. G.; Langen, R.; Lanyi, J. K. *Biochemistry* **2012**, *51*, 1051.

(19) Chen, G. Q.; Gouaux, E. *Biochemistry* **1999**, *38*, 15380.

(20) Schlebach, J. P.; Kim, M.-S.; Joh, N. H.; Bowie, J. U.; Park, C. *J. Mol. Biol.* **2011**, *406*, 545.

(21) Ikai, A.; Tanford, C. *J. Mol. Biol.* **1973**, *73*, 145.

(22) Cao, Z.; Schlebach, J. P.; Park, C.; Bowie, J. U. *Biochim. Biophys. Acta, Biomembr.* **2012**, *1818*, 1049.

(23) Chang, Y.-C.; Bowie, J. U. *Proc. Natl. Acad. Sci. U. S. A.* **2014**, *111*, 219.

(24) De Los Rios, M. A.; Muralidhara, B. K.; Wildes, D.; Sosnick, T. R.; Marqusee, S.; Wittung-Stafshede, P.; Plaxco, K. W.; Ruczinski, I. *Protein Sci.* **2006**, *15*, 553.

(25) Booth, P. J.; Riley, M. L.; Flitsch, S. L.; Templer, R. H.; Farooq, A.; Curran, A. R.; Chadborn, N.; Wright, P. *Biochemistry* **1997**, *36*, 197.

(26) Booth, P. J. *Folding Des.* **1997**, *2*, R85.

(27) Krishnamani, V.; Lanyi, J. K. *Biophys. J.* **2011**, *100*, 1559.

(28) Pan, Y.; Brown, L.; Konermann, L. *J. Mol. Biol.* **2011**, *410*, 146.

(29) Khanal, A.; Pan, Y.; Brown, L. S.; Konermann, L. *J. Mass Spectrom.* **2012**, *47*, 1620.

(30) Popot, J.-L.; Engelman, D. M. *Biochemistry* **1990**, *29*, 4031.

(31) Makarov, D. E. *Protein Sci.* **2003**, *12*, 17.

(32) Luecke, H.; Schobert, B.; Richter, H.-T.; Cartailler, J.-P.; Lanyi, J. K. *J. Mol. Biol.* **1999**, *291*, 899.

(33) Hong, H.; Blois, T. M.; Cao, Z.; Bowie, J. U. *Proc. Natl. Acad. Sci. U. S. A.* **2010**, *107*, 19802.

(34) Faham, S.; Yang, D.; Bare, E.; Yohannan, S.; Whitelegge, J. P.; Bowie, J. U. *J. Mol. Biol.* **2004**, *335*, 297.

(35) Cline, S. W.; Doolittle, W. F. *J. Bacteriol.* **1987**, *169*, 1341.

(36) Oesterhelt, D.; Stoeckenius, W. *Methods Enzym.* **1974**, *31*, 667.